Pressure dependence of metallization and superconducting transition in AgCl and AgBr

2004 J. Phys.: Condens. Matter 16 1577

(http://iopscience.iop.org/0953-8984/16/9/006)

INSTITUTE OF PHYSICS PUBLISHING JOURNAL OF PHYSICS: CONDENSED MATTER

J. Phys.: Condens. Matter **16** (2004) 1577–1592 PII: S0953-8984(04)69426-4

Pressure dependence of metallization and superconducting transition in AgCl and AgBr

C Nirmala Louis, K Iyakutti[1] and P Malarvizhi

Department of Microprocessor and Computer, School of Physics, Madurai Kamaraj University, Madurai 625 021, Tamil Nadu, India

E-mail: iyakutti@yahoo.co.in

Received 23 September 2003
Published 20 February 2004
Online at stacks.iop.org/JPhysCM/16/1577 (DOI: 10.1088/0953-8984/16/9/006)

Abstract

The electronic band structure, metallization, structural phase transition and superconducting transition of silver chloride (AgCl) and silver bromide (AgBr) under pressure are studied using the TB-LMTO method. The ground state properties and bandgap values are compared with the experimental and previous theoretical results. These silver halides become metals and superconductors under high pressure, but before this they undergo structural phase transition from NaCl phase to CsCl phase. It is found that the charge transfers between Ag 5s, 4d and X np, nd (X = Cl, Br; $n = 3, 4$) states cause metallization. It is found that the metallization pressure increases with decrease of lattice constant. The density of states at the Fermi level ($N(E_F)$) is enhanced as the pressure is further increased, which leads to the superconductivity in AgCl and AgBr. Like CsI, AgCl and AgBr come under the class of pressure induced superconductors. The pressure effects on λ (electron–phonon mass enhancement factor) and μ^* (electron–electron interaction parameter) clearly suggest that AgCl and AgBr are electron–phonon mediated superconductors. The non-occurrence of metallization, phase transition and onset of superconductivity simultaneously in ionic solids is also confirmed.

1. Introduction

Silver chloride and silver bromide, which crystallize in NaCl structure under ambient conditions, are of great physical interest in normal and high pressure investigations; since they act as photographic materials, solid electrolytes and liquid semiconductors [1]. The recent development in the diamond anvil cell [2, 3] enables the experimentalist to reach a very high value of pressure. The increase of pressure means a significant decrease in volume, which results in a change of electronic states and crystal structure. Experimentally, it is

[1] Author to whom any correspondence should be addressed.

found that the ionic compound CsI is a metal under high pressure, and as the pressure is increased superconductivity sets in [3]. These results lead us to expect superconductivity in other ionic compounds under high pressure, especially those compounds which have already become metals. Subjecting silver halides to high pressure leads to pressure induced structural phase transition, semiconductor–metal transition and superconducting transition at megabar pressures. The structural phase transition and electronic structure of silver halide compounds under high pressure is a popular topic in condensed matter research [4–8].

There are many experimental and theoretical investigations related to the band structure and phase transition of AgCl and AgBr [9–39]. The pressure induced structural phase transitions in silver halides have been experimentally observed by Hull and Keen [5] and Kusada *et al* [39]. Recently, the experimental investigation on phase relations of AgI under high pressure and high temperature were reported by Ohtaka *et al* [9]. On the theoretical side, very recently, Okoye [4] has presented the structural properties and electronic band structure of silver halides at normal pressure using the full potential linearized augmented plane wave (FP-LAPW) method within the local density approximation (LDA) and the generalized gradient approximation (GGA). Also, Jochym and Parlinski [11] studied the elastic properties and phase stability of AgBr under pressure using density functional theory (DFT) with pseudopotentials and GGA. Among the various theoretical studies, the structural phase transition in silver halides was predicted by Gupta and Singh [12] using the three-body potential (TBP) method, followed by Nunes and Allen [6] using the LDA with a pseudopotential plane wave method. Similarly, various groups [1, 4, 8, 13–24] have investigated the band structure of silver halides under normal pressure. It is felt that many important parameters are involved in these calculations and further theoretical studies are needed to improve the agreement with the experiment [5, 10].

In all the above studies, only very little information is provided about the high pressure behaviour (structural phase transition) of AgCl and AgBr. In particular, no work has been reported regarding the high pressure electronic band structure, metallization or superconducting transition of silver halides. In view of this, attempt is made to obtain the

(i) normal pressure band structure and density of states (with NaCl structure) and
(ii) high pressure band structure and density of states (with CsCl structure),

and analyse the structural phase transition from NaCl to CsCl, metallization and superconducting transition (with CsCl structure). The high pressure band structures corresponding to metallization and onset of superconducting transition, which have not been available previously, are displayed.

In section 2, the details of the calculational procedure, electronic band structure and density of states corresponding to normal and high pressures are given. The ground state properties, structural phase transition, metallization, superconducting transition temperature T_c and its variation under pressure are discussed in section 3. Concluding remarks are given in section 4.

2. Electronic structure

2.1. Method of calculation

The band structure and the density of states are computed using the first principles tight binding linear muffin-tin orbital (TB-LMTO) method within the local density approximation (LDA) and atomic sphere approximation (ASA) [40]. The computational details of the TB-LMTO method are well described in the literature [40–42]. The exchange–correlation potential within the LDA is included using the parametrization scheme of von Barth and Hedin [43]. The total and partial density of states are calculated by the tetrahedron method [44]. All relativistic

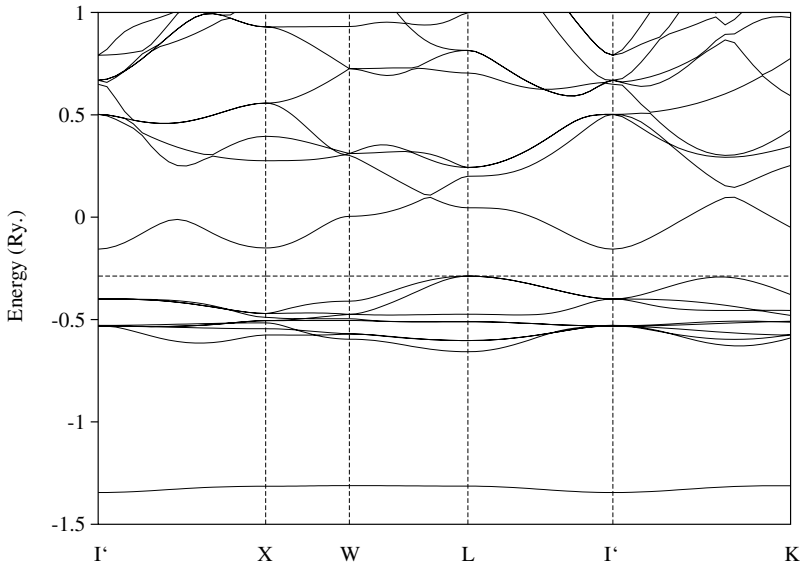

Figure 1. Band structure of AgCl at $V/V_0 = 1$.

corrections except spin–orbit coupling are included. The entire Brillouin zone is partitioned into 4096 cubical volume elements and $E(k)$ is computed for the k-point located at the centre of the each volume element. But because of the symmetry considerations this involves only 145 k-points and 165 k-points for NaCl and CsCl structures respectively. The Wigner–Seitz sphere radii are chosen in such a way that the sphere boundary potential is minimum and the charge flow between the atoms is according to the electronegativity criteria [41]. The overlaps of the atomic spheres for the different structures are less than 4%. The included combined correction terms correct the error due to the non-spherical shape of the atomic shells and the truncation of higher partial waves inside the sphere. The self-consistency iterations were continued until the total energy difference between two consecutive iterations was less than 10^{-5} Ryd. The electronic configurations of Ag, Cl and Br are [Kr] $4d^{10}5s^1$ ($Z = 47$), [Ne] $3s^23p^5$ ($Z = 17$) and [Ar] $3d^{10}4s^24p^5$ ($Z = 35$) respectively. The valence electronic configurations chosen in our calculation are $5s^14d^{10}$ for Ag, $3s^23p^5$ for Cl and $4s^24p^5$ for Br. Throughout the calculation there are 18 valence electrons for AgCl and AgBr.

2.2. Band structure and density of states

The band structures and density of states of AgCl and AgBr are calculated for various reduced volumes ranging from $V/V_0 = 1.0$ to 0.3 in steps of 0.05 for both NaCl and CsCl structures (figures 1–8). The band structures are given along the symmetry directions Γ–X–W–L–Γ–K for the NaCl structure (figure 1) and Γ–H–N–Γ–P–N for the CsCl structure (figures 3, 5, 7 and 8).

Normal pressure. The overall topology of the band structure at normal pressure (figure 1) is similar to the previous calculations [1, 4, 13–24, 45]. The 3s electrons of Cl atom form a narrow band which is positioned at the bottom of the valence band (figure 1). This feature is in agreement with the theoretical calculation of Vogel *et al* [13]. The remaining eight bands appearing just below the Fermi energy E_F (figure 1) are due to Ag 5s, 4d and Cl 3p states of

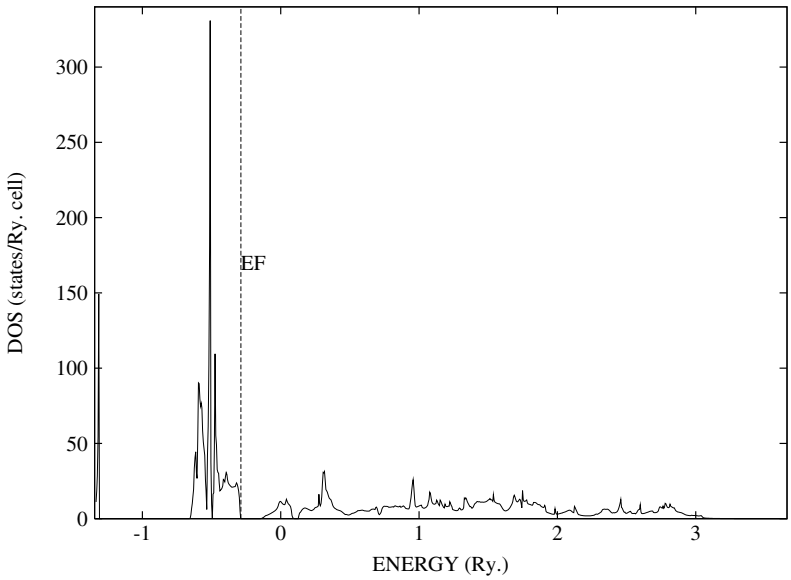

Figure 2. Density of states of AgCl at $V/V_0 = 1.0$.

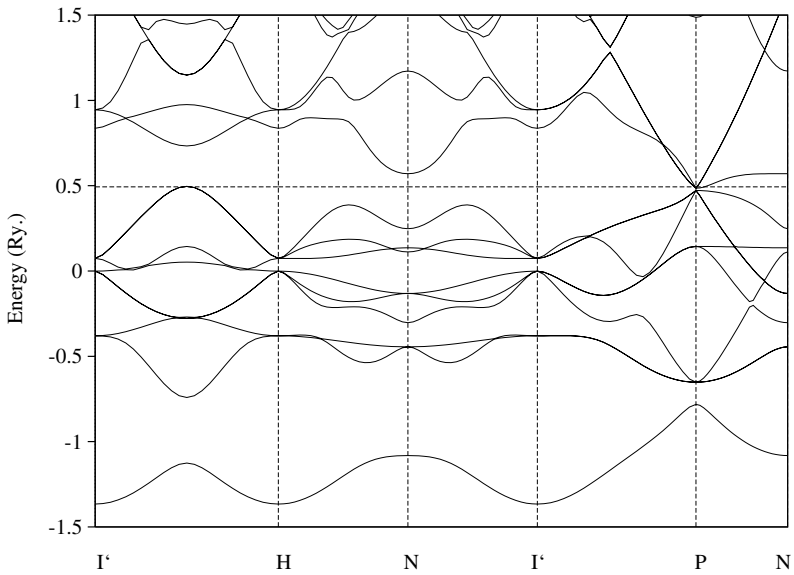

Figure 3. Band structure of AgCl at $V/V_0 = 0.476$.

AgCl. In figure 1, the empty conduction bands above the Fermi energy are due to Ag 5p, Cl 4s3d states. The lowest conduction band is derived mainly from the mixture of Ag 5s and Cl 3p states [4].

The band structure of AgBr is very similar to that of AgCl [46, 47]. In particular, Br 4s electrons have approximately the same energy relative to the Cl 3s electrons. There are no significant differences between the band structure of AgCl and AgBr, therefore we have not displayed the band structure of AgBr. In our calculation, regarding the relative positions of

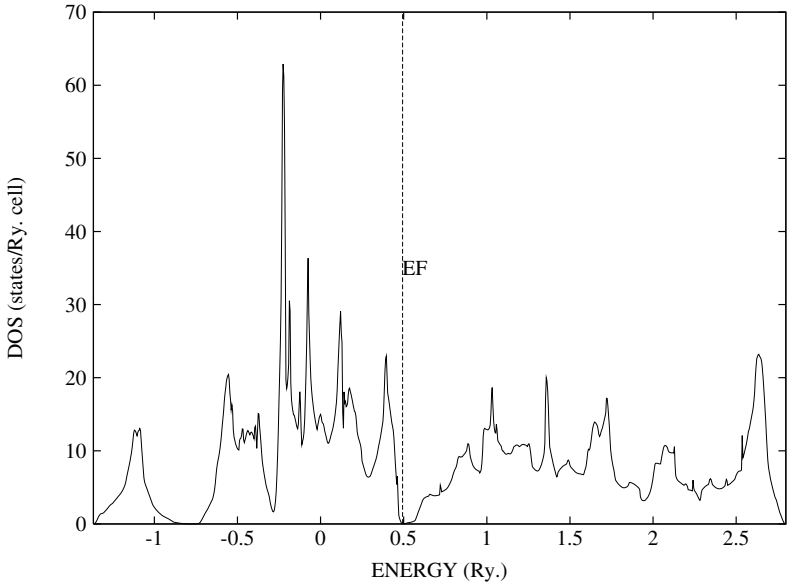

Figure 4. Density of states of AgCl at $V/V_0 = 0.476$.

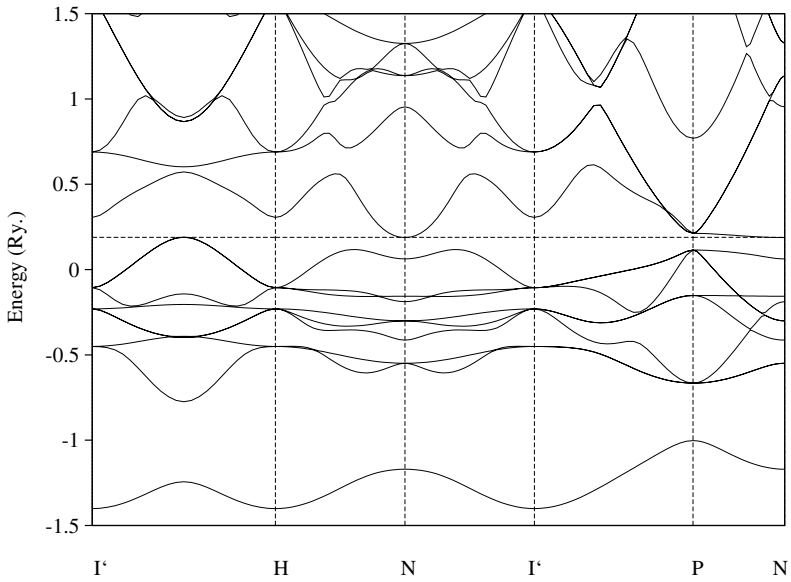

Figure 5. Band structure of AgBr at $V/V_0 = 0.488$.

the Ag d level and Cl, Br p levels, it is found that the X^- np level (X = Cl, Br; $n = 3, 4$) lies somewhat above the Ag^+ 4d level, which is similar to the results already reported [13–24]. The presence of cation 4d levels in the valence region produces strong hybridization with anion p levels. This strong hybridization leads to a covalent contribution to the chemical bond, indirect energy gap and large valence band width in AgCl and AgBr at normal pressure [7, 15]. These features are well brought out in our calculations.

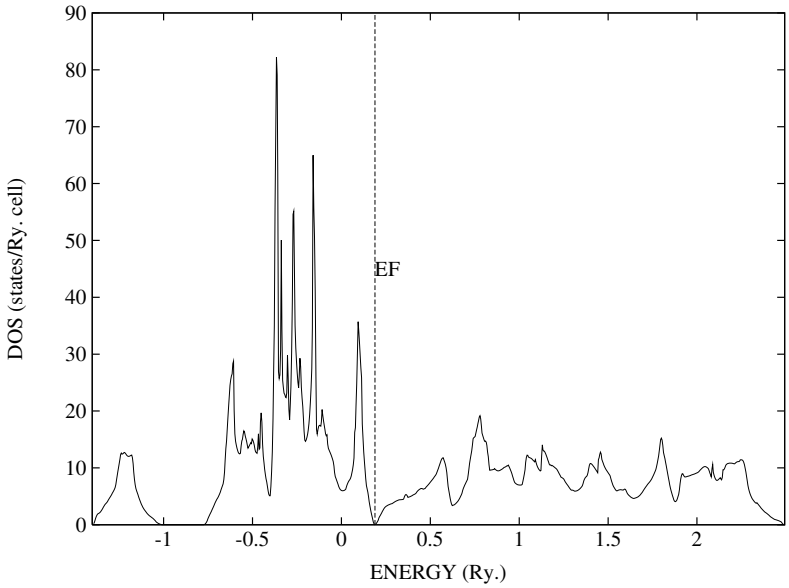

Figure 6. Density of states of AgBr at $V/V_0 = 0.488$.

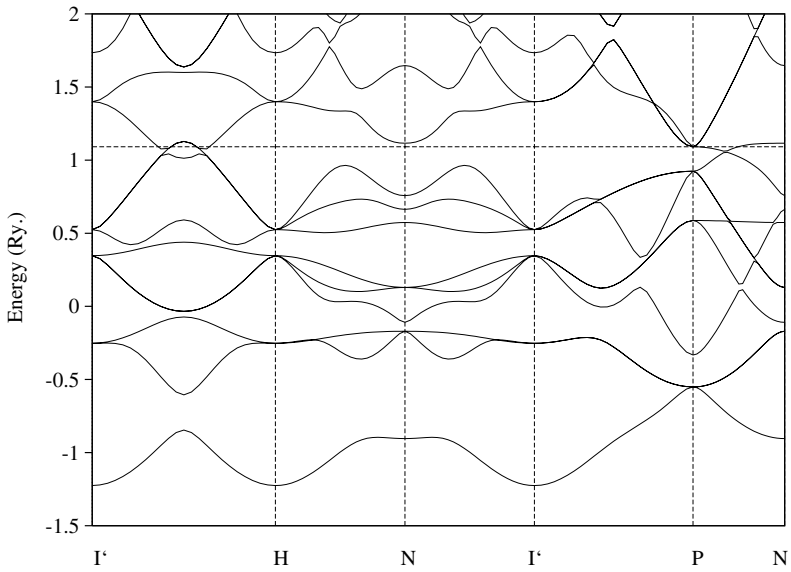

Figure 7. Band structure of AgCl at $V/V_0 = 0.375$.

At normal pressure, the bandgap is indirect with the top of the valence band occurring at the L-point and the bottom of the conduction band at the Γ-point (figure 1). The values of the direct bandgap at the Γ-point ($E_g\Gamma$–Γ), the indirect bandgap (E_gL–Γ) and the valence band width (VBW L–L) of eight bands appearing just below the Fermi energy E_F are given in table 1 along with the experimental [7–10] and previous theoretical values [1, 4, 13–24]. The calculated energy gaps are in agreement with the previous LDA values [1, 16] for both

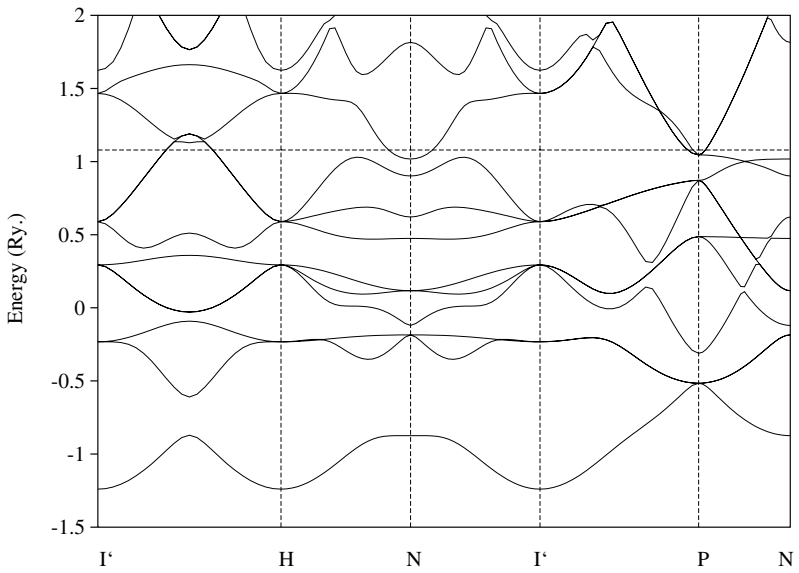

Figure 8. Band structure of AgBr at $V/V_0 = 0.375$.

AgCl and AgBr (table 1). But compared to the experimental value, the LDA underestimates the bandgap.

The density of states (DOS) histogram of AgCl at normal pressure is shown in figure 2. It is seen that at normal pressure the levels arising from Cl 3s states give a long spike near the origin. The highest spike near the Fermi energy is due to Ag 5s, 4d and Cl 3p states. The short peaks above the Fermi energy E_F are due to the 5p state of Ag and 4s3d states of Cl [4, 7, 15]. Since the density of states of AgBr is similar to AgCl, we have not given the histogram of AgBr at normal pressure. The narrow peaks near the origin for both AgCl and AgBr are mainly of halogen s states. The high peaks in AgCl and AgBr, probably originating from the region around the Γ-point in the Brillouin zone, are similar to the peaks given in the previous calculation [4]. This peak in figure 2 is proof of the strong hybridization between Ag 4d and halogen p states. Above the Fermi level, the broad bumps originate from the Ag p state as well as the halogen d state [15]. The general features of the band structure and density of states (figures 1 and 2) are similar to those of the alkali halides [41], but in silver halides Ag 4d electrons are involved.

High pressure. Since AgCl and AgBr are ionic semiconductors, they are characterized by wide bandgap at ambient conditions [5, 13]. Under the application of pressure, AgCl and AgBr undergo first order structural phase transitions from sixfold coordinated NaCl structure to eightfold coordinated CsCl structure [6–12, 36–38]. This was experimentally observed by Hull and Keen [5] and Kusada *et al* [39]. So to compute the high pressure band structure and density of states, we have chosen the CsCl structure as the stable structure for AgCl and AgBr (figures 3–8). As pressure increases, the entire band structure is slowly shifted up in energy and the valence bandwidth increases. This is because of the enhanced overlapping of the wavefunctions with the neighbouring atoms. Under pressure, the tight binding character of individual bands is enhanced but the overlapping disperses the bands, increasing the overall valence bandwidth. Visible changes are seen in the band structures of AgCl and AgBr at

Table 1. The values of direct bandgap ($E_g\Gamma$–Γ), indirect bandgap (E_gL–Γ) and valence band width (VBW L–L) of AgCl and AgBr.

Silver halide	AgCl			AgBr		
Energy gap	$E_g\Gamma$–Γ (eV)	E_gL–Γ (eV)	VBW L–L (eV)	$E_g\Gamma$–Γ (eV)	E_gL–Γ (eV)	VBW L–L (eV)
Present work TB-LMTO	3.404	1.620	5.037	3.185	1.382	5.239
Experiment [8, 10, 7]	5.20 [8] 5.60 [10]	3.25 [10] 3.00 [21]	5.90 [10]	4.30 [13]	2.90 [8] 2.70 [7] 2.68 [10] 2.50 [21]	5.90 [10]
DFT-LDA [1]	3.5	1.25	5.48	—	—	—
LASTO-LDA [16]	3.6	1.3	5.3	3.0	1.3	5.1
LMTO-ASA KKR [8]	4.21	3.19	—	3.69	2.94	—
DFT-Xα [18]	5.69	3.77	4.12	—	—	—
APW [23]	5.13	3.84 3.28	—	4.29	3.24 2.89	—
FP-LAPW GGA [4]	3.221	0.935	—	2.546	0.694	—
FP-LAPW LDA [4]	2.909	0.633	—	2.247	0.394	—
Hartree–Fock [35]	15.4	13.5	6.18	—	—	—
SIRC-PP [13]	4.5	2.3	5.4	3.1	3.1	5.4
NC-PP [13]	2.8	0.6	5.5	1.9	0.1	5.5
Others	4.3 [10] 5.47 [24] 5.17 [32]	3.2 [10] 3.71 [24] 3.17 [32]	—	5.5 [14] 4.22 [24]	1.0 [15] 3.23 [24]	—

Γ-points corresponding to different high pressures (figures 3, 5, 7 and 8), since the electronic system is strongly coupled to the lattice under pressure.

Electrons in s, p and d shells of Ag, Cl and Br as a function of different reduced volumes are given in tables 2 and 3 for AgCl and AgBr respectively (NaCl structure and CsCl structure). There is charge transfer, between Ag 5s, 4d and X-np, nd (X = Cl, Br; $n = 3, 4$) bands, which varies with increase of pressure. In our calculation, at $V/V_0 = 1$, nearly 0.54 electrons are transferred from the Ag 5s state to the Cl 3p state (table 2) and 0.31 electrons are transferred from the Ag 5s state to the Br 4p state (table 3). The charge distributions due to the above transfers in AgCl and AgBr indicate that the bonding is of ionic character under normal conditions and AgCl is more ionic than AgBr [5, 13]. As the compounds are compressed, the Ag 5s electron density goes on increasing, whereas Cl 3p and Br 4p electron density decreases (tables 2 and 3). This indicates that the bonding between silver and halogen atoms becomes less ionic or more covalent under compression. Simultaneously, the number of Ag 4d electrons goes on decreasing under pressure whereas the halogen d electron number is increasing, which leads to metallization and superconductivity.

The increase of pressure causes the broadening of bands which results in the decrease of density of state value in most of the energy regions of the DOS histogram. Thus in figures 4 and 6, the heights of the spikes are considerably reduced. When pressure increases E_F increases whereas no density of states is available at the Fermi level up to metallization pressure. There are appreciable values for DOS at $V/V_0 = 0.476$ (figure 4) and $V/V_0 = 0.488$ (figure 6) for AgCl and AgBr respectively, indicating metallization. Further increase in pressure leads to

Table 2. Electrons in s, p and d shells of Ag and Cl at different reduced volumes in NaCl structure ($V/V_0 = 1.0$ to 0.8) and CsCl structure ($V/V_0 = 0.793$ to 0.3).

		Ag			Cl		
V/V_0	P (Mbar)	$5s^1$	$5p^0$	$4d^{10}$	$3s^2$	$3p^5$	$3d^0$
1.0	Normal	0.468	0.142	9.526	1.871	5.539	0.454
0.9	0.081	0.500	0.154	9.448	1.847	5.536	0.515
0.8	0.210	0.538	0.168	9.350	1.818	5.531	0.594
0.793	0.221	0.360	0.413	9.839	1.972	5.168	0.248
0.7	0.419	0.377	0.463	9.780	1.959	5.107	0.313
0.6	0.770	0.393	0.522	9.699	1.941	5.039	0.404
0.5	1.370	0.409	0.592	9.588	1.915	4.963	0.531
0.4	2.489	0.426	0.721	9.331	1.854	4.816	0.850
0.3	4.508	0.437	0.801	9.089	1.801	4.635	1.235

Table 3. Electrons in s, p and d shells of Ag and Br at different reduced volumes in NaCl structure ($V/V_0 = 1.0$ to 0.9) and CsCl structure ($V/V_0 = 0.808$ to 0.3).

		Ag			Br		
V/V_0	P (Mbar)	$5s^1$	$5p^0$	$4d^{10}$	$4s^2$	$4p^5$	$4d^0$
1.0	Normal	0.543	0.160	9.678	1.843	5.310	0.464
0.9	0.073	0.578	0.175	9.610	1.813	5.301	0.523
0.808	0.183	0.423	0.487	9.919	1.971	4.967	0.233
0.7	0.390	0.443	0.554	9.868	1.955	4.878	0.301
0.6	0.719	0.462	0.624	9.807	1.934	4.790	0.382
0.5	1.297	0.479	0.706	9.725	1.905	4.692	0.492
0.4	2.367	0.501	0.806	9.609	1.864	4.561	0.659
0.3	4.398	0.524	0.909	9.457	1.807	4.385	0.917

enhanced density of states at the Fermi level, which induces superconductivity in AgCl and AgBr (figures 7 and 8).

3. Results and discussion

3.1. Ground state properties

The ground state properties and structural phase transitions of AgCl and AgBr are analysed using the total energies calculated as a function of reduced volume (V/V_0) for both B1 (NaCl) and B2 (CsCl) phases of AgCl and AgBr. From the total energies, it is found that the ground state structure of AgCl and AgBr is NaCl as observed experimentally and reported from other theoretical calculations [4–39] and at high pressure NaCl structure is transformed into CsCl (B2) structure [4, 5, 11, 12]. The calculated total energies are fitted to the Birch–Murnaghan equation of state [48],

$$P = 1.5B_0[(V_0/V)^{7/3} - (V_0/V)^{5/3}][1 + 0.75(B_0^1 - 4)\{(V_0/V)^{2/3} - 1\}] \quad (1)$$

to obtain the equilibrium volume V_0 (and hence the equilibrium lattice constant a_0) and other ground state properties. The calculated pressures under various reduced volumes of AgCl and AgBr are given in tables 2 and 3 respectively. The equilibrium lattice constant, bulk modulus and its pressure derivative are tabulated in table 4 along with the experimental [5, 25–30] and previous theoretical values [1, 4, 6–13]. From table 4, it is observed that one gets larger

Table 4. Equilibrium lattice constant (a_0), bulk modulus (B_0) and its pressure derivative (B_0^1) for AgCl and AgBr.

	AgCl			AgBr		
Ground state properties	Present work	Experimental works	Previous theoretical works	Present work	Experimental works	Previous theoretical works
a_0 (au)	10.429	10.492 [26] 10.488 [5] 10.485 [25]	10.608 [4] 10.109 [4] 10.227 [6] 10.321 [1] 10.189 [13] 10.454 [13]	10.851	10.937 [11] 10.916 [25] 10.870 [26]	11.013 [4] 10.544 [4] 10.662 [6] 10.488 [1] 10.548 [13] 10.794 [13]
B_0 (Mbar)	0.644	0.513 [28] 0.470 [5]	0.620 [1] 0.668 [6] 0.670 [4] 0.440 [4]	0.595	0.450 [5] 0.410 [29]	0.513 [1] 0.603 [6] 0.632 [4] 0.396 [4] 0.426 [11]
B_0^1	3.469	5.980 [27] 0.400 [5]	5.200 [6] 5.396 [4] 5.410 [4]	5.500	0.400 [5] 8.500 [30]	5.100 [6] 5.293 [4] 7.147 [4]

lattice constant corresponding to smaller bulk modulus. This arises because the compressibility decreases as the size of the anion decreases [6]. This is the general trend in alkali halides [41], which is confirmed now for silver halides AgCl and AgBr.

3.2. Structural phase transitions

There are many experimental and theoretical studies regarding the phase stability of AgCl and AgBr [5–12, 36]. Nunes and Allen [6] investigated the energies of the several possible structures and proposed an intermediate trigonal cinnabar phase which is present in between NaCl and CsCl phases. In contrast to this Hull and Keen [5], with the help of their experimental work, suggested that an intermediate phase with a monoclinic KOH type is present in between the NaCl and CsCl phases of silver halides. Recently in AgBr, a KOH type structure has been predicted theoretically by Jochym and Parlinski [11]. In their investigation, NaCl structure is found to be stable up to 0.08 Mbar and the KOH phase becomes more stable in the pressure interval 0.08–0.35 Mbar. Above 0.35 Mbar CsCl type structure is the most stable one. Thus in silver halides monoclinic KOH type structure is the transformation path from NaCl to CsCl structure [5, 11]. Now for AgCl and AgBr, above normal pressure we have considered only the CsCl structure [5, 6, 11, 12], because in this study we are interested in the non-metal to metal transition and superconducting transition of AgCl and AgBr which occur above 1.0 Mbar.

Before metallization and superconducting transition, like other ionic compounds with NaCl structure [41], AgCl and AgBr also undergo a phase transition to the CsCl structure [5]. The phase stability of NaCl and CsCl structures of AgCl and AgBr is analysed using the enthalpy calculation. The enthalpy is defined by

$$H(P) = E_{\text{tot}}(P) + PV(P) \tag{2}$$

and the transition pressure corresponding to the phase change from B1 (NaCl) to B2 (CsCl) is obtained from the relation

$$H_{\text{B1}}(P) = H_{\text{B2}}(P) \tag{3}$$

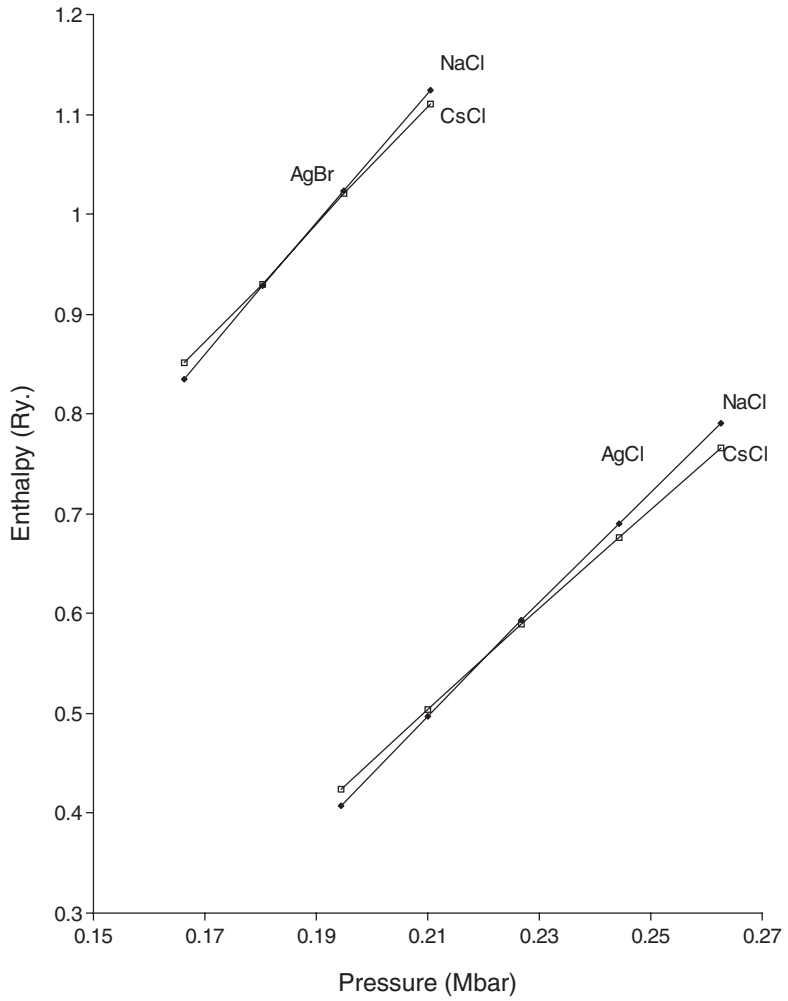

Figure 9. Enthalpy versus pressure curve for AgCl and AgBr.

where H_{B1} and H_{B2} are the enthalpies of the B1 and B2 phases respectively. The enthalpy versus pressure plots of AgCl and AgBr are given in figure 9. The phase transition pressures (P_T) for AgCl and AgBr estimated by solving the above equations (equations (2) and (3)) are given in table 5 along with the available experimental [5, 36] and other theoretical results [6, 11, 12].

For AgBr our calculated phase transition pressure is in good agreement with the previous theory [6], whereas a considerable difference exists in the case of AgCl (table 5). Our calculated values are higher than the experimental value of Slykhouse and Drickamar [36], but our results support the hypothesis formulated by Hull and Keen [5] that 'P_T for NaCl to CsCl transition is greater than 0.161 Mbar for AgCl and 0.127 Mbar for AgBr'.

3.3. Metallization

It is well known that many ionic solids undergo insulator to metal transition upon applying high pressure [3, 41]. Most of these metallizations are associated with a structural transition from a low coordination non-metallic to a high coordination metallic phase. At normal pressure,

Table 5. NaCl to CsCl phase transition pressure (P_T) in AgCl and AgBr.

NaCl–CsCl transition	AgCl P_T (Mbar)	AgBr P_T (Mbar)
Present study	0.221	0.183
Experiments	>0.165 [5]	>0.127 [5]
	0.087 [36]	0.083 [36]
Previous theoretical works	0.110 [6]	>0.350 [11]
	0.079 [12]	0.170 [6]
		0.073 [12]

Table 6. Comparison of metallization, phase transition and superconducting transition in AgCl and AgBr.

	Metallization		Phase transition		Onset of superconducting transition	
Silver halide	P_M (Mbar)	$(V/V_0)_M$	P_T (Mbar)	$(V/V_0)_T$	P_S (Mbar)	$(V/V_0)_S$
AgCl	1.588	0.476	0.221	0.793	2.891	0.375
AgBr	1.393	0.488	0.183	0.808	2.762	0.375

AgCl and AgBr are indirect wide bandgap semiconductors [1, 4]. The fundamental energy gap (L–Γ) is between the filled p-like valence band due to halogen and empty s-like conduction band due to silver (figure 1). The bandgap values are 1.62 and 1.382 eV for AgCl and AgBr respectively.

As the pressure is increased, there is a continuous electron transfer which leads to the increase in the 5s electron number of silver and d electron number of halogen. This causes an increase in the width of the valence and conduction bands. All these lead to the decrease in the energy gap and finally metallization in AgCl and AgBr. The band structures corresponding to metallization of AgCl and AgBr are shown in figures 3 and 5 respectively. The indirect bandgap semiconductors at ambient pressure can become metals by direct or indirect band overlap [41]. In AgCl, the metallization takes place by the indirect closure (figure 3) of the bandgap between the Cl 3p-like valence band (in between Γ- and H-points) and the Ag 5s-like conduction band (at the P-point). The metallization pressure (P_M) of AgCl is 1.588 Mbar, which corresponds to the reduced volume (V/V_0) 0.476 (table 6).

In AgBr, the indirect closure (figure 5) of bandgap between the Br 4p-like valence band and the Ag 5s-like conduction band (the valence band maximum is in between Γ- and H-points and the conduction band minimum is at the N-point) occurs at the pressure (P_M) of 1.393 Mbar, which corresponds to the reduced volume (V/V_0) 0.488 (table 6). Due to pressure the localized Ag 4d electrons are transferred to the halide d state, where these d electrons are relatively free (itinerant) compared to their earlier status. As a result metallization sets in in silver halides. Similar to alkali halides, the electronic band structure calculations on silver halides suggest that metallization is due to the reordering of the energy bands with the empty s-like band (silver) dropping in energy and touching the top of the filled p-like bands (halogen). However, there is no experimental or theoretical study for comparison at these pressures.

The metallization pressure calculated for AgCl is greater than that of AgBr (table 6). This means that in silver halides metallization pressure increases with decreasing size of the anion ($Cl^- = 3.421$ au and $Br^- = 3.705$ au). This trend is similar to the trend observed in alkali

halides having NaCl structure at ambient conditions [41]. The reason for this similarity is that prior to metallization both alkali halides and silver halides undergo structural transition from NaCl to CsCl structure [38]. At the metallization pressures, the values for density of states at Fermi energy $N(E_F)$ are very small, which indicates that metallization has just set in in AgCl (figure 4) and in AgBr (figure 6). Thereafter $N(E_F)$ increases slowly with pressure and becomes fairly large at a particular value of V/V_0. The values of E_F and $N(E_F)$ corresponding to different V/V_0 values are used in studying the pressure variation of superconducting transition temperature [42].

3.4. Superconductivity under pressure

All ionic solids would become superconductors due to high compression [3, 49]. The continuous promotion of s, p electrons to d shells in solids under pressure is one of the factors which will induce superconductivity [49]. Under very high pressure, silver halides are not only metals but also superconductors. The theory of Gaspari and Gyorffy in conjunction with McMillan's formula is used to calculate T_c [50, 51].

The electron–phonon mass enhancement factor (λ) is

$$\lambda = \frac{N(E_F)\langle I^2\rangle}{M\langle\omega^2\rangle} \tag{4}$$

where M is the atomic mass, $\langle\omega^2\rangle$ is an average of the phonon frequency square and $\langle I^2\rangle$ is an average (over the Fermi energy) of the electron–phonon matrix element square. $\langle I^2\rangle$ (in Rydbergs) can be written as [42, 49]

$$\langle I^2\rangle = 2\sum_l \frac{(l+1)}{(2l+1)(2l+3)} M_{l,l+1}^2 \frac{N_l(E_F)N_{l+1}(E_F)}{N(E_F)N(E_F)} \tag{5}$$

where $M_{l,l+1} = -\phi_l\phi_{l+1}[(D_l(E_F)-1)(D_{l+1}(E_F)+l+2)+(E_F-V(S))S^2]$ and here ϕ_l is the radial wavefunction at the muffin-tin sphere radius corresponding to the Fermi energy. D_l is the logarithmic derivative of the radial wavefunction at the sphere boundary. $V(S)$ is the muffin-tin potential at the sphere boundary. S is the radius of the muffin-tin sphere. The above quantities are taken from the band structure results [42, 49]. We have calculated λ separately for silver and halide atoms and for the T_c-calculation (equation (8)) the mean value of λ is used [49].

The average of the phonon frequency square is approximated as

$$\langle\omega^2\rangle = \tfrac{1}{2}\theta_D^2. \tag{6}$$

The variation of Debye temperature with pressure $\theta_D(P)$ is given by [42, 49, 52]

$$\theta_D(P) = \frac{\sqrt{E_F}}{\sqrt{E_F^0}}\frac{a_0}{a}\theta_D^0 \tag{7}$$

where θ_D^0, a_0 and E_F^0 are normal pressure quantities. θ_D^0 for Ag, Cl, Br, AgCl and AgBr is 215, 115, 110, 163 and 121 K respectively [53].

McMillan's formula [50],

$$T_c = \frac{\theta_D}{1.45}\exp\left[\frac{-1.04(1+\lambda)}{\lambda-\mu^*(1+0.62\lambda)}\right] \tag{8}$$

gives a good estimate of the T_c-value [42]. Here μ^* is the electron–electron interaction parameter which is estimated using the relation [54]

$$\mu^* = \frac{0.26N(E_F)}{1+N(E_F)} \tag{9}$$

where $N(E_F)$ is the density of levels per atom per electronvolt at E_F.

Table 7. T_c-values as a function of pressure for AgCl in CsCl structure.

Pressure P (Mbar)	Density of states $N(E_F)$ (states/Ryd cell)	λ	θ_D (K)	μ^*	T_c (K)
2.8910	0.1817	0.0835	716.3	0.0034	0.0004
3.3583	0.5194	0.2054	770.6	0.0096	0.8473
3.8973	0.6497	0.2387	833.2	0.0118	1.8785
4.5080	0.7555	0.2509	905.9	0.0137	2.4673

Table 8. T_c-values as a function of pressure for AgBr in CsCl structure.

Pressure P (Mbar)	Density of states $N(E_F)$ (states/Ryd cell)	λ	θ_D (K)	μ^*	T_c (K)
2.7620	3.9715	0.1684	515.0	0.0588	0.0028
3.2252	4.4061	0.2188	554.0	0.0636	0.0670
3.7690	4.4870	0.2431	598.2	0.0645	0.1953
4.3990	4.6523	0.2827	649.1	0.0663	0.6641

With these results we have analysed the variation of θ_D, λ, μ^* and T_c with pressure using equations (4)–(9) [42, 49]. The calculated values for θ_D, λ, μ^* and T_c under various pressures are given in table 7 (for AgCl) and table 8 (for AgBr). Irrespective of the size of the halide atom (anion), silver halides AgCl and AgBr start superconducting at the same V/V_0-value (0.375) (table 6). From tables 7 and 8, it is seen that T_c increases with increase of pressure and reaches a maximum value of 2.47 K for AgCl at 4.5 Mbar and 0.66 K for AgBr at 4.4 Mbar. The onset of superconductivity in AgCl occurs at 2.89 Mbar and thereafter T_c increases with the pressure coefficient of 1.53 K Mbar^{-1}. In the case of AgBr, the onset of superconductivity occurs at 2.76 Mbar and thereafter T_c increases with the pressure coefficient of 0.404 K Mbar^{-1}. Our study reveals that in the case of silver halides the Ag s band overlaps with halogen p bands (figures 7 and 8) and some of the Ag 4d and Cl, Br p electrons go over to the d shell of Cl and Br in such a way that there is an increase in $N(E_F)$ at $V/V_0 = 0.375$, which promotes superconductivity. This is the characteristic feature of ionic solids [3, 49]. Our theoretical estimate for μ^* (tables 7 and 8) is small when compared to the standard value ($\mu^* = 0.1$) used for metals. This is because the DOS at $E_F(N(E_F))$ on which μ^* depends (equation (9)) is zero to start with and increases slowly with pressure in silver halides. We have calculated the pressure dependence of Debye temperature $\theta_D(P)$ using equation (7). Even though it is an extrapolation of measured Debye temperature at normal pressure, the $E_F(P)$-values are calculated from the band structure results corresponding to pressure P.

The path to the enhancement of T_c under pressure lies in the direction of higher $\theta_D(P)$. Also the pressure dependence of electron–electron interaction parameter μ^* increases slightly with pressure whereas electron–phonon mass enhancement factor λ increases significantly with pressure. The calculated T_c values depend more sensitively on the changes in λ and μ^*. But the contribution from $\mu^*(P)$ to the variation of $T_c(P)$ is much less important than that of $\lambda(P)$ [55]. From tables 7 and 8 we concluded that AgCl and AgBr are electron–phonon mediated superconductors. The calculated λ-values of AgCl and AgBr are small (tables 7 and 8), thus one can expect measurable superconductivity at low temperature as we have predicted. A similar situation was observed in CsI both experimentally [3] and theoretically [49]. The growth of the halogen d-electron number with pressure is higher in

AgCl than AgBr (tables 2 and 3). This may be the reason for the appreciable value of T_c (2.47 K) in AgCl at 4.5 Mbar when compared to AgBr (0.66 K at 4.4 Mbar). This T_c-value in AgCl is attributed to the itinerant nature of Cl 3d electrons which are promoted from the Ag 4d and Cl 3p states. From this, we concluded that silver halides are pressure induced superconductors with low T_c-values.

4. Conclusion

In summary, we have investigated the high pressure band structure, density of states, metallization and superconducting transition in AgCl and AgBr (in CsCl structure). The structural phase transition from NaCl to CsCl is found to occur at 0.221 Mbar for AgCl and 0.183 Mbar for AgBr. The calculated ground state properties of AgCl and AgBr are in better agreement with the experimental observation than the previous theoretical calculations. The broadening of both the valence and conduction bands with pressure leads to the bandgap closure and the formation of metallic states at 1.588 Mbar in AgCl and 1.393 Mbar in AgBr. The metallization pressure of AgCl is greater than that of AgBr, which indicates that when the size of the anion decreases the pressure required for metallization increases [41]. As the external pressure is further increased, the density of states at the Fermi level $N(E_F)$ increases due to charge transfer leading to superconducting transition in AgCl and AgBr. The calculated T_c-values, pressure variation of λ (electron–phonon mass enhancement factor) and μ^* (electron–electron interaction parameter) lead us to conclude that AgCl and AgBr are electron–phonon mediated superconductors. The pressures corresponding to structural phase transition, metallization and onset of superconductivity decrease when the lattice constant increases (table 6). This is because the compressibility increases as the size of the anion increases. It is also confirmed that metallization, phase transition and superconductivity do not occur simultaneously in silver halides. Even though there is no experimental evidence now, we hope to get the experimental results soon as in the case of CsI.

Acknowledgments

We thank the University Grants Commission (UGC) for the special assistance under UGC-DRS and COSIST.

References

[1] Kirchhoff F, Holender J M and Gillan M J 1994 *Phys. Rev.* B **49** 17420
[2] Lindbaum A, Heathman S, Litfin K and Meresse Y 2001 *Phys. Rev.* B **63** 214101
[3] Eremets M I, Shimizu K and Amaya K 1998 *Science* **281** 1333
[4] Okoye C M I 2002 *Phys. Status Solidi* b **234** 580
[5] Hull S and Keen D A 1999 *Phys. Rev.* B **59** 750
[6] Nunes G S and Allen P B 1998 *Phys. Rev.* B **57** 5098
[7] Mason M G, Tan Y T, Miller T J, Kwawer G N, Brown F C and Kunz A B 1990 *Phys. Rev.* B **42** 2996
[8] Ves S, Glotzel D, Cardona M and Overhof H 1981 *Phys. Rev.* B **24** 3073
[9] Ohtaka O, Takebe H, Yoshiasa A, Fukui H and Katayama Y 2002 *Solid State Commun.* **123** 213
[10] Tejada T, Shevchik N J, Braun W, Goldmann A and Cardona M 1975 *Phys. Rev.* B **12** 1557
[11] Jochym P T and Parlinski K 2001 *Phys. Rev.* B **65** 024106
[12] Gupta D C and Singh R K 1991 *Phys. Rev.* B **43** 11185
[13] Vogel D, Kruger P and Pollmann J 1998 *Phys. Rev.* B **58** 3865
[14] Kunz A B 1982 *Phys. Rev.* B **26** 2070
[15] Onwuagba B N 1996 *Solid State Commun.* **97** 267
[16] Victora R H 1997 *Phys. Rev.* B **56** 4417

[17] Nunes G S, Allen P B and Martins J L 1998 *Solid State Commun.* **105** 377
[18] Gordienko A, Zhuravlev N Yu and Poplavnoi A S 1991 *Phys. Status Solidi* b **168** 149
[19] Stefanovich E, Dovesi R and Roetti C 1991 *Chem. Phys. Lett.* **186** 329
[20] Bosani F, Knox R S and Fowler W B 1965 *Phys. Rev.* **137** 1217
[21] Sommer A H 1968 *Photoemissive Materials* Ist edn (NewYork: Wiley) chapter 3, p 21
[22] De Boer P K and De Groot R A 1999 *J. Phys. Chem.* A **103** 5113
[23] Scop P M 1965 *Phys. Rev.* **139** A934
[24] Fowler A B 1972 *Phys. Status Solidi* b **52** 591
[25] Berry C 1955 *Phys. Rev.* **97** 676
[26] Wyckoff R W 1968 *Crystal Structures* (NewYork: Wiley)
[27] Lawactz P 1972 *Phys. Rev.* B **5** 4039
[28] Hidshaw W, Lewis J T and Briscoe C V 1967 *Phys. Rev.* **163** 876
[29] Tannhouser D S, Bruner L J and Lawson A W 1956 *Phys. Rev.* **102** 1281
[30] Vaidya S N and Kennedy G C 1971 *J. Phys. Chem. Solids* **32** 951
[31] Hohenberg P and Kohn W 1964 *Phys. Rev.* **136** B864
[32] Wang S-Y J, Schluter M and Cohen M L 1976 *Phys. Status Solidi* b **77** 295
[33] Farberovich O V, Timoshenko Y K, Bugakov A M and Domashevskaya E P 1981 *Solid State Commun.* **40** 559
[34] Kunz A B 1982 *Phys. Rev.* B **26** 2070
[35] Apra E, Stefanovich E, Dovesi R and Roetti C 1991 *Chem. Phys. Lett.* **186** 329
[36] Slykhouse T E and Drickamar H G 1958 *J. Phys. Chem. Solids* **7** 207
[37] Mason M G 1975 *Phys. Rev.* B **11** 5094
[38] Toledano P, Knorr K, Ehm L and Depmeier W 2003 *Phys. Rev.* B **67** 144106
[39] Kusada K, Syono Y, Kikegawa T and Shimomura O 1995 *J. Phys. Chem. Solids* **56** 751
[40] Anderson O K and Jepson O 1984 *Phys. Rev. Lett.* **53** 2571
Anderson O K 1975 *Phys. Rev.* B **12** 3060
[41] Nirmala Louis C and Iyakutti K 2002 *Phys. Status Solidi* b **233** 339
[42] Nirmala Louis C and Iyakutti K 2003 *Phys. Rev.* B **67** 094509
[43] von Barth U and Hedin L 1972 *J. Phys. C: Solid State Phys.* **5** 1629
[44] Anderson O K and Jepson O 1971 *Solid State Commun.* **9** 1763
[45] Nirmala Louis C and Iyakutti K 2002 *DAE-Solid State Physics Symp. (Panjab University, Chandigarh, India)* p 92 (Abstract)
[46] Malarvizhi P, Nirmala Louis C and Iyakutti K 2002 *DAE-Solid State Physics Symp. (Panjab University, Chandigarh, India)* p 92 (Abstract)
[47] Malarvizhi P 2002 *MPhil Thesis* Madurai Kamaraj University
[48] Murnaghan F D 1944 *Proc. Natl Acad. Sci. USA* **30** 244
[49] Nirmala Louis C and Iyakutti K 2003 *Phys. Status Solidi* b **236** 614
[50] McMillan W L 1968 *Phys. Rev.* **167** 331
[51] Gaspari G D and Gyorffy B L 1972 *Phys. Rev. Lett.* **29** 801
[52] Ashcroft N W and Mermin N D 1981 *Solid State Physics* (Philadelphia, PA: Saunders) p 512
[53] Bruesch P 1982 *Phonons—Theory and Experiments* vol 1 (Berlin: Springer) p 81
[54] Bennemann K H and Garland J W 1972 *AIP Conf. Proc.* **4** 103
[55] Chen X J, Zhang H and Habermeier H U 2002 *Phys. Rev.* B **65** 144514